



OSSE for a sustainable marine observing network in the Sea of Marmara

Ali Aydođdu^{1,2,3}, Timothy J. Hoar⁴, Tomislava Vukicevic⁵, Jeffrey L. Anderson⁴, Nadia Pinardi^{6,7}, Alicia Karspeck⁴, Jonathan Hendricks⁴, Nancy Collins⁴, Francesca Macchia⁸, and Emin Özsoy⁹

¹Science and Management of Climate Change, Ca' Foscari University of Venice, Italy

²Centro Euro-Mediterraneo sui Cambiamenti Climatici, Bologna, Italy

³Nansen Environmental and Remote Sensing Center, Bergen, Norway

⁴National Center for Atmospheric Research, Boulder, Colorado, USA

⁵Office of Water Prediction, National Weather Service NOAA, Tuscaloosa, Alabama, USA

⁶Department of Physics and Astronomy, University of Bologna, Italy

⁷Istituto Nazionale di Geofisica e Vulcanologia, Bologna, Italy

⁸Barcelona Supercomputing Center (BSC), Barcelona, Spain

⁹Eurasia Institute of Earth Sciences, Istanbul Technical University, Turkey

Correspondence: Ali Aydođdu (ali.aydogdu@nersc.no)

Received: 17 December 2017 – Discussion started: 4 January 2018

Revised: 15 May 2018 – Accepted: 12 June 2018 – Published: 27 July 2018

Abstract. An observing system simulation experiment (OSSE) is presented in the Sea of Marmara. A high-resolution ocean circulation model (FESOM) and an ensemble data assimilation tool (DART) are coupled. The OSSE methodology is used to assess the possible impact of a FerryBox network in the eastern Sea of Marmara. A reference experiment without assimilation is performed. Then, synthetic temperature and salinity observations are assimilated along the track of the ferries in the second experiment. The results suggest that a FerryBox network in the Sea of Marmara has potential to improve the forecasts significantly. The salinity and temperature errors get smaller in the upper layer of the water column. The impact of the assimilation is negligible in the lower layer due to the strong stratification. The circulation in the Sea of Marmara, particularly the Bosphorus outflow, helps to propagate the error reduction towards the western basin where no assimilation is performed. Overall, the proposed FerryBox network can be a good start to designing an optimal sustained marine observing network in the Sea of Marmara for assimilation purposes.

1 Introduction

The Sea of Marmara is one of the compartments of a water passage known as the Turkish Straits System (hereafter TSS). The TSS connects the Black Sea and the Mediterranean by two narrow straits, namely the Bosphorus and the Dardanelles, along with the Sea of Marmara.

Salty and dense Mediterranean waters and brackish Black Sea waters form a two-layer exchange flow through the TSS. In combination with the complex topography, flow structures on different scales generate a challenging environment for oceanographic studies.

Until recently, building a model to solve the hydrodynamics of the complete TSS was not considered a feasible undertaking due to high computational costs of the required horizontal and vertical resolution enabling the representation of the sharp stratification and the extremely complex topography of the straits and shelf regions, largely differing from those of the larger neighboring basins. However, models with increasing computational capacity to model the whole system have emerged in recent years (Sannino et al., 2017; Gürses et al., 2016; Stanev et al., 2017).

In this study we present, to the best of our knowledge, the first data assimilation experiments performed in the Sea of Marmara. In the region, in situ observations are generally

scarce and collected by dedicated projects (Ünlüata et al., 1990; Özsoy et al., 2001; Beşiktepe et al., 1994; Tuğrul et al., 2002; Chiggiato et al., 2012) for a limited area and time. Moreover, the spatial resolution and frequency of satellite observations are still not sufficient to monitor the system continuously. For these reasons, a sustainable marine monitoring network is required in the Sea of Marmara. We propose a FerryBox network mounted on existing public transportation infrastructure.

We follow the observing system simulation experiment (OSSE) methodology to achieve our goal. OSSE has been used widely in the atmospheric community for 4 decades to design new observation tools, for error assessment in large models and for parameter estimation (Arnold Jr. and Dey, 1986; Masutani et al., 2010). Atlas (1997) summarizes the criteria established by the atmospheric community to perform credible OSSE. Halliwell Jr. et al. (2014, 2015) gave an example of an ocean OSSE in the Gulf of Mexico by following those criteria. Aydođdu et al. (2016) studied a fishery-observing system in the Adriatic Sea, taking the same criteria into account.

This paper is organized as follows: in the next section, the main characteristics of the TSS relevant to this study are summarized. In Sect. 3, the model and data assimilation scheme that we used are documented. Section 4 is devoted to the OSSE design. The nature run and forward model are introduced. FerryBox network design is also detailed and the methodology for impact assessment is outlined. The results are discussed in Sect. 5. The summary and conclusions are presented in the last section.

2 Overview of the Turkish Straits System

The Sea of Marmara with the Bosphorus and the Dardanelles straits constitute the Turkish Straits System, which connects the Black Sea and the Mediterranean. The exchange of contrasting water masses forms a highly stratified water column structure throughout the system with a pycnocline around 20 m depth. The brackish surface water of the Black Sea flows towards the Mediterranean in the upper layer and the salty and dense Mediterranean Sea water occupies the lower layer of the water column (Ünlüata et al., 1990). In addition to the strong stratification, the complex topography of the two narrow straits and an internal sea with shallow shelves and deep depressions presents a unique and challenging environment for oceanographic studies.

The Bosphorus is an elongated narrow strait connecting the Black Sea and the Sea of Marmara. The upper layer flow is dominated by the Black Sea water, with salinity of about 18 psu. The lower layer water originates in the Mediterranean and reaches the Black Sea with a salinity of about 37 psu. The interface depth between the two layers is mainly determined by the salinity gradient. In summer, a three-layer temperature structure appears. A warm upper layer due to the atmospheric

heat flux overlays a cold intermediate layer that propagates from the Black Sea. Warmer Mediterranean water constitutes the bottom layer (Altıok et al., 2012). The constriction in the midsection and the sill in the southern section of the strait apply a hydraulic control on the flow and produce a surface jet at the Sea of Marmara exit (Sözer and Özsoy, 2017). The velocity of the Bosphorus jet can exceed 2 m s^{-1} (Jarosz et al., 2011). Therefore, the jet is one of the key factors influencing the dynamics of the Sea of Marmara. It enhances the mixing by entraining lower layer water (Ünlüata et al., 1990), energizes the Sea of Marmara circulation in the eastern basin (Beşiktepe et al., 1994) and produces mesoscale eddies due to the potential vorticity balance (Sannino et al., 2017).

The wind is another important factor influencing the dynamics of the Sea of Marmara. Many strong cyclones pass over the Sea of Marmara, especially in winter (Book et al., 2014). Northeasterly winds dominate the atmospheric circulation throughout the year.

The third important dynamical constituent is the density-driven baroclinic flow in the lower layer (Hüsrevođlu, 1998). The velocity of the flow in the lower layer can reach 1 m s^{-1} (Jarosz et al., 2012).

The high complexity of the system requires models that simultaneously solve the whole system in its smallest resolved details and optimally represent multiple scales of interest.

3 Ensemble modeling and data assimilation in the TSS

The ocean model used in this study is the Finite Element Sea-ice Ocean Model (FESOM). FESOM is an unstructured mesh ocean model using finite element methods to solve the hydrostatic primitive equations with the Boussinesq approximation (Danilov et al., 2004; Wang et al., 2008). Gürses et al. (2016) applied FESOM to the TSS and performed realistic simulations of the complete system using atmospheric forcing. The TSS model domain extends zonally from 22.5 to 33° E and meridionally from 38.7 to 43° N . The mesh resolution is as fine as 65 m in the Bosphorus and 150 m in the Dardanelles. In the Sea of Marmara, the resolution is always finer than 1.6 km and is not coarser than 5 km in the Black Sea and the Aegean Sea. The water column is discretized by 110 vertical z levels. Vertical resolution is 1 m in the first 50 m depth and increases to 65 m at the bottom boundary layer in the deepest part of the model domain. The mesh has 70 240 nodes at the surface layer and more than 3 million nodes for the 3-D state variables i.e., temperature, salinity, zonal and meridional velocity.

Aydođdu (2017) performed interannual simulations using a similar model setup. Two 6-year simulations using different surface salinity boundary conditions have been completed and evaluated. It is shown that the model is able to simulate main characteristics of the system qualitatively. It simulates the two-layer structure of the TSS, successfully. Moreover, dynamical properties such as sea level difference be-

tween different compartments and dynamics related to high-frequency atmospheric events are well captured. However, the error growth in temperature and salinity throughout the simulation is also demonstrated, which motivates the need for data assimilation in the TSS.

In this study FESOM has been coupled with an ensemble-based data assimilation framework, Data Assimilation Research Testbed (DART). DART is an open-source community facility developed at NCAR (Anderson et al., 2009) that provides data assimilation tools to work with either low-order or high-order models for different research activities (Raeder et al., 2012; Karspeck et al., 2013; Schwartz et al., 2015; Hoteit et al., 2013).

DART includes several different stochastic and deterministic ensemble Kalman filtering algorithms. In this study, we use the ensemble adjustment Kalman filter (EAKF) as described in Anderson (2001). The EAKF is a deterministic ensemble Kalman filter, where the observations are not perturbed randomly before they are assimilated. One of the main advantages of the EAKF for our application is that it preserves the prior covariance distribution during resampling, which is not the case for the ensemble filters such as kernel or Gaussian resampling filters. The ensemble covariance is used to quantify the relation between pairs of state variables or an observation and a state variable in the linear Gaussian context of the ensemble Kalman filter. In other words, it is the statistical representation of the prior constraints (dynamical balances) generated by the model. For a linear model, a sufficiently large ensemble would be able to represent all the balances. However, our model is nonlinear and cost forces us to use a small ensemble. This means that the ensemble sample covariances do not exactly represent the dynamical balances. The ensemble filter algorithm and inflation we use are designed to maintain the prior ensemble covariance as much as possible. Moreover, localization is effective in reducing forecast root mean square error (RMSE) compared to observations, given the errors in the sample covariances. However, it disrupts the prior sample covariance, so can result in reduced dynamical balance. In the TSS, where different dynamics compete and generate circulation structures at various scales, the prior distribution is crucial for maintaining the dynamical balances among different scales, which justifies the choice of the EAKF. In addition, analysis covariances are updated in every assimilation cycle, which is important to sustain the high-frequency variability of the system.

One of the main issues to take into consideration in ensemble data assimilation is the filter divergence. It can result from insufficient ensemble variance, which leads to assigning more weight to the prior information that in turn may cause rejection of information from observations. As a result, the analysis departs from the observations (Anderson, 2001). There are techniques to prevent filter divergence such as inflating the covariances (Anderson and Anderson, 1999). In the standard DART, inflation of the prior ensemble leads to multiplying the prior covariances by a constant slightly

larger than 1. Instead of DART's multiplicative covariance inflation, we have applied random perturbations to the background vertical diffusivity for each ensemble member since one of the main sources of error in the model is the vertical mixing and the position of the interface between the upper and lower layers. The background vertical diffusivity κ_{v_0} , which is implicitly represented in the κ_v of the tracer equations, is randomly perturbed all over the domain every time step by fitting a Gaussian distribution, with a mean of 0 and a standard deviation of 5 % of the κ_{v_0} . We note that κ_{v_0} is approximately 2 orders of magnitude smaller than the spatially and temporally varying κ_v .

Houtekamer and Mitchell (1998) show that spurious correlations in the prior information can be avoided by using large ensembles. Since it is computationally expensive to use large ensembles in large geophysical models, they proposed a spatial localization technique to overcome spurious small correlations associated with remote observations. The impact of an observation on state variables is reduced as a function of distance from the observation, with impact going to zero at a finite cutoff value. In DART, the cutoff value can be set as a constant value in radians. The localization function is the fifth-order piecewise continuous function, compactly supported as presented in Gaspari and Cohn (1999). The horizontal cutoff radius, which is the half-width of the Gaspari–Cohn kernel, is used to deal with the high spatial variability of the water masses along the TSS. Moreover, the water column in the TSS is strongly stratified in the vertical. Therefore, vertical localization is also applied to update the state in the upper layer of the water column, with less impact in the lower layer. As a result, the localization is an ellipsoidal volume centered on the observation being assimilated, with a horizontal radius of two cutoff values and vertical radius of two cutoff values normalized by a factor. This approach is chosen to avoid problems such as the breaking of the stratification during the integration.

For interfacing FESOM and DART, a forward operator that maps model state vector into observation space, characterized by a type of physical quantity, georeferenced location and time were defined. For the FerryBox type of observations we used a simple, but theoretically justifiable nearest-neighbor mapping. Specifically, for each discrete observation value the forward operator first finds the closest horizontal grid point in the state vector and then the closest vertical location.

The details of the FESOM–DART coupling are shown schematically in Fig. 1. The interface to DART requires two model-specific routines that convert the model restart files to DART state vectors and vice versa. For the model-to-DART step the state vector is provided from each ensemble member. The updated state vectors are then converted to the model restart files as an initial ensemble for the next assimilation cycle within which FESOM is applied to integrate the model state forward to the next analysis time. This process is repeated until the experiment finishes.

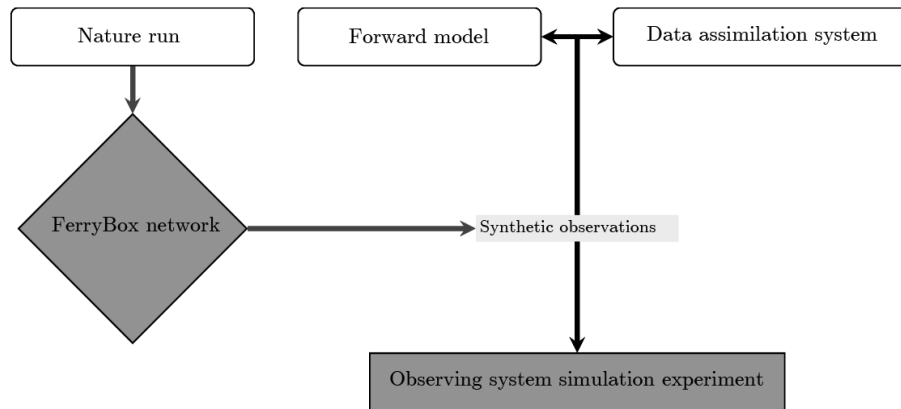


Figure 2. OSSE methodology applied in the Turkish Straits System. The forward model (FM) is a different configuration of the model setup used for the nature run (NR) as detailed in the text.

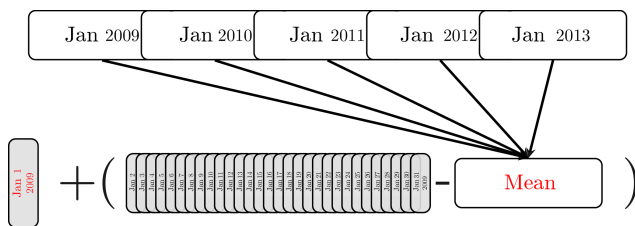


Figure 3. Schematic representation of the methodology used to generate the initial ensemble. MEAN is the January averages over 5 years between 2009 and 2013.

(<http://www.ferrybox.org>, last access: June 2018), especially in the northern European seas. In the Mediterranean, there is a FerryBox system between Piraeus and Heraklion (Korres et al., 2014) operated by Hellenic Centre for Marine Research (HCMR). A FerryBox mainly includes temperature, salinity, turbidity and chlorophyll *a* fluorescence sensors, as well as a GPS receiver for measuring position. Oxygen, pH, $p\text{CO}_2$ or algal groups as well as air pressure, air temperature and wind sensors can also be installed (Petersen, 2014). The FerryBox observations can be used for analyzing the state of the ocean (Seppälä et al., 2007) and comparison with other instruments (Sørensen et al., 2007) and can also be assimilated to improve the state of the ocean models (Grayek et al., 2011).

The sampling rate of the data can vary between systems. The data used in Grayek et al. (2011) are sampled at 10 s intervals. For our OSSE, we use a sampling rate of 1 min following Korres et al. (2014). The synthetic observations are obtained from hourly NR outputs at varying spatial locations so as to remain within 1 min time intervals along the track of the ferries. The depth of the sampling is set to 5 m, an average depth given by Grayek et al. (2011). A random error, sampled by a Gaussian distribution around zero mean and standard deviation of 0.1 °C for temperature and 0.04 psu for salinity, is added to each synthetic observation following

Aydođdu et al. (2016) in order to simulate realistic measurements, taking the instrumental error into account. These synthetic observations are the same for each ensemble member; i.e., the Kalman filtering is not stochastic in which observations are perturbed. Moreover, observational error matrices in the Kalman gain are chosen to be uncorrelated and constant diagonal, with 0.5 °C and 0.25 psu for temperature and salinity, respectively, as proposed by Grayek et al. (2011) while considering other sources of error such as representativeness.

Three different ferry routes are chosen from the map in Fig. 5a, and their tracks are approximated by observing from the real-time Marine Traffic (<https://www.marinetraffic.com>, last access: June 2018) application (Fig. 5b). The longest duration for a cruise in the eastern Sea of Marmara is about 3.5 h between Ambarlı and Topçular (Table 1). Another transect used here is YeniKapı–Yalova, which takes about 75 min and has cruises every 2 h from each port. This route directly crosses the Bosphorus outflow and has the highest number of cruises a day. Therefore, we include six ferries in various periods of the day for YeniKapı–Yalova transect. The last transect chosen is Yenikapı–Bandırma, which crosses the Sea of Marmara from north to south. The navigation on this line takes about 2.5 h. This transect is the only one that has direct impact in the southern basin. The resulting synthetic temperature and salinity observations sampled from the NR for the first day are shown in Fig. 6.

4.3 Experiments

Two experiments are performed as an initial evaluation for the data assimilation studies in the Sea of Marmara (Table 2). The first experiment FB001 is a reference experiment without assimilation. It is used to evaluate the errors when the synthetic observations are not assimilated. In the second experiment, FB002, all the synthetic observations are assimilated in the corresponding assimilation window. A 6 h width is chosen for each assimilation window, since the area is un-

Table 1. The unidirectional ferry tracks used in this study. The locations, distance between the ports, speed of the ferries, duration of the cruise and time of departure from each port are listed.

Route	Location	Distance	Speed	Duration	Departure time (UTC)
Yenikapı – Yalova	41.002° N, 28.956° E 40.661° N, 29.274° E	46.2 km (28.7 mi.)	23 kn	75 min	09:45, 15:45, 21:45 07:15, 13:45, 19:45
Yenikapı – Bandırma	41.002° N, 28.956° E 40.354° N, 27.967° E	110.0 km (68.5 mi.)	27 kn	150 min	07:30 18:30
Ambarlı – Topçular	40.966° N, 28.676° E 40.690° N, 29.434° E	70.0 km (43.2 mi.)	12 kn	210 min	20:00 16:00

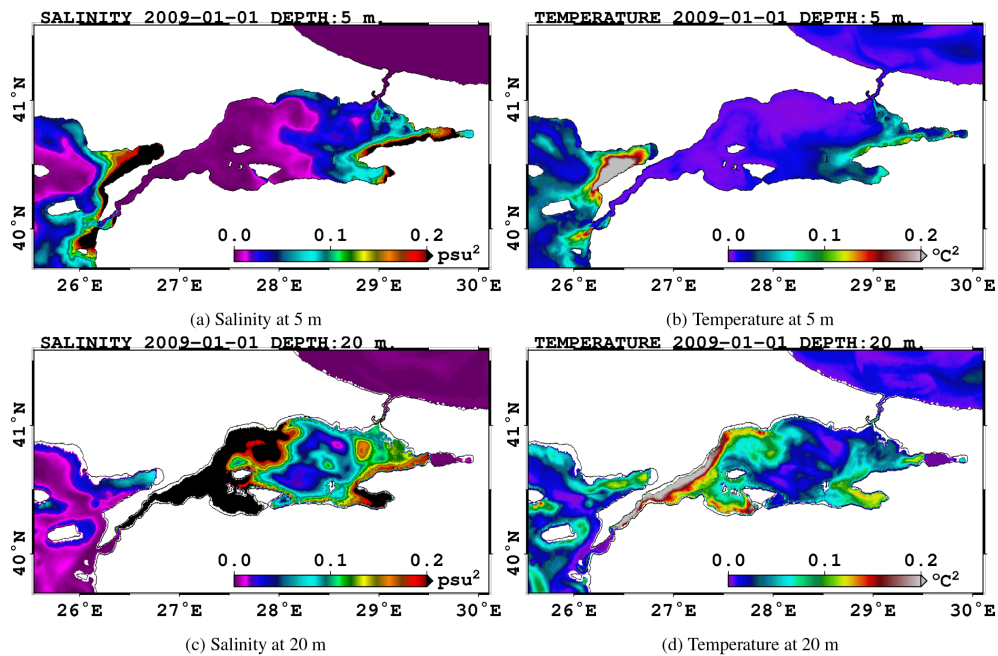


Figure 4. Salinity (a, c) and temperature (b, d) variance of the initial ensemble at 5 m (a, b) and 20 m (c, d) depth on 1 January 2009 at 00:00 UTC.

Table 2. Summary of the OSSEs. Start and end date of both experiments are the same. There is no assimilation in FB001 whereas all the data are assimilated in FB002. Assimilation cycle is 6 h for FB002.

	Start date	End date	Assimilation	A. cycle	Evaluation
FB001	1 Jan 2009 00:00	8 Jan 2009 00:00	None	n/a	Yes
FB002	1 Jan 2009 00:00	8 Jan 2009 00:00	All	6 h	Yes

n/a: not applicable

der the influence of the Bosphorus jet, which may develop high-frequency variability in the water mass structure and circulation at the upper layer, especially during severe storms and atmospheric cyclone passages.

The horizontal cutoff radius is set to 6.36 km and the vertical cutoff radius is considered as 15 m centered on the observation location. The mean temperature and salinity increments after the first and third assimilation cycle are shown in Fig. 7a and b, respectively. As can be seen from the temper-

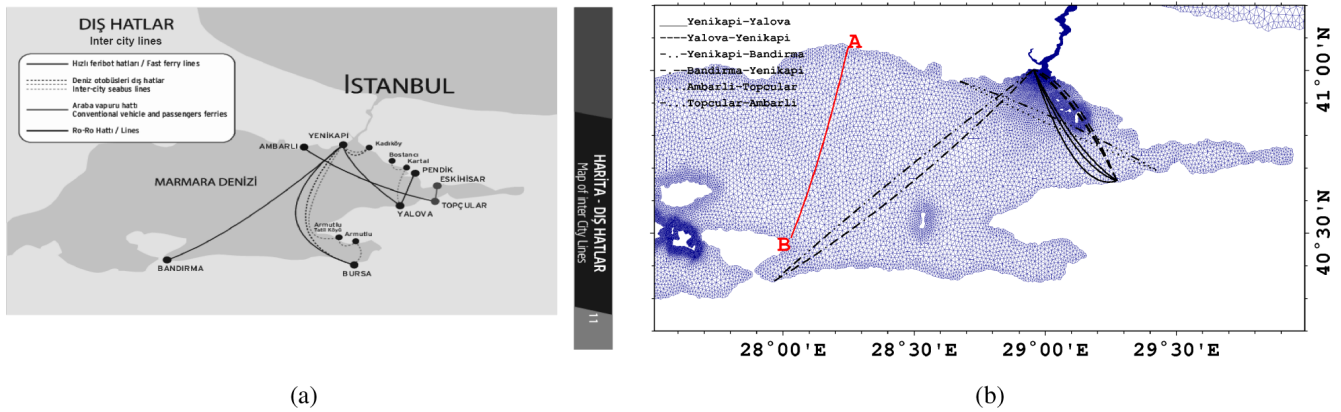


Figure 5. (a) The routes of the intercity ferry lines from Istanbul and to Istanbul suggested by the operating company IDO (<http://www.ido.com.tr>, last access: June 2018). (b) Approximate unidirectional ferry tracks. The legend shows the direction of the ferries. The section A–B is used only for impact assessment against the NR. Triangular mesh of the model is underlaid.

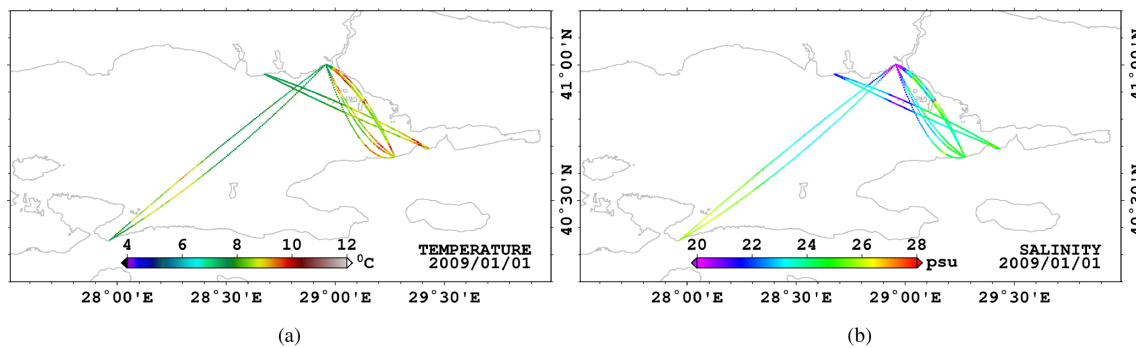


Figure 6. Synthetic (a) temperature and (b) salinity observations on 1 January 2009 sampled from the NR.

ature corrections after the first cycle, the whole track of the Yenikapi–Bandırma route is not assimilated at the same time since the southern section of the data is not in the current assimilation window. Moreover, the updates on the salinity fields are smaller around 20 m (Fig. 7b), compared to the upper layers (not shown) closer to the observation locations.

4.4 Methodology for impact assessment

The DART offers tools to have the control of the data without any difficulty. Each type of observation can either be assimilated or withheld to evaluate the resulting analyses. DART also provides a rudimentary quality control capability that can reject observations that are too different from the ensemble mean prior estimate. Synthetic observations are not used in the assimilation (rejected) if $x_b - y > TE(x_b - y)$. Here, y is the observation and x_b is the corresponding prior mean of the ensemble of forward operators. The expected value, E , is computed as follows:

$$E(x_b - y) = \sqrt{\sigma_{x_b}^2 + \sigma_y^2}, \quad (1)$$

where σ stands for the standard deviation. T is chosen as 3 for both temperature and salinity in these experiments, considering the real model errors reported by Aydođdu (2017).

The first diagnostic we use to assess the impact of the observations is the root mean square of innovations, which are the root mean square of the difference between the prior and observation. We also use horizontal maps of the innovations to determine the spatial distribution of error.

The OSSE methodology enables various ways of evaluating the analysis since the NR is assumed to be the true state of the system. We exploit this assumption to compare the experiments with the NR to understand the impact of assimilation better.

One diagnostic we use in this sense is the comparison between the NR and ensemble mean in the vertical. Although we do not assimilate any data below 5 m and we limit the radius for vertical updates, it is important to assess the vertical distribution of the errors given the strongly stratified water column in the Sea of Marmara. For this purpose, we compute the difference between prior ensemble mean and NR along the transect A–B (see Fig. 5) in the first 50 m depth.

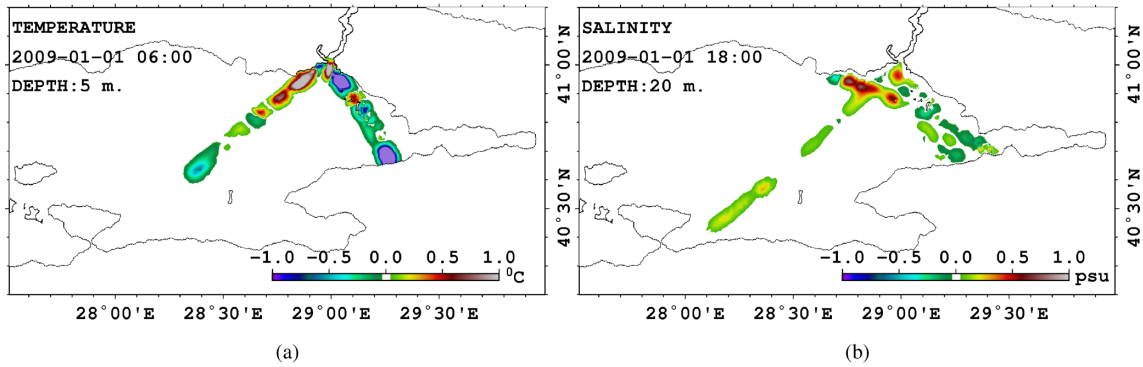


Figure 7. Mean increments after assimilation for (a) temperature at 1 January 2009 at 06:00 UTC at 5 m depth and (b) salinity at 1 January 2009 18:00 UTC at 20 m depth.

The second diagnostic is the root mean square (RMS) of difference between the prior ensemble mean and the NR computed in the first 10 m of the water column for the whole basin. The propagation of the error reduction can be traced from the spatial maps of this diagnostic.

5 Results

Figure 8 shows the time evolution of prior RMS of innovations, ensemble spread and total spread for temperature and salinity. The RMS of salinity innovations continuously grows in FB001. It fluctuates around 2 psu and reaches 2.4 psu at the end of sixth day. In FB002, assimilation of the observations decreases the RMS of innovations significantly. The RMS of innovations is generally below 1.2 psu. Although there is an increase of error in the first 2 days, a gradual reduction takes place in the following days. The RMS of temperature innovations behaves similarly to that of salinity after the second day. The error grows in FB001 even though the trend is not as obvious as in salinity errors of the same experiment. The analysis is improved at the end of experiment FB002 compared to FB001. The range of errors is comparable to the real model errors with respect to in situ observations, as demonstrated by Aydođdu (2017). Another important result is that the ensemble still has spread comparable to the RMSEs at the end of the experiments (larger in FB001). In other words, the ensemble did not collapse after a week of assimilation. We recall that the ensemble spread is maintained by perturbing the background vertical diffusivity. The method seems promising at least for a week-long period.

As discussed in Sect. 4.4, the data are subjected to a quality control before assimilation. Figure 8c and d show the number of available observations (N_{poss}), number of used observations (N_{used}) and number of outlier observations (N_{out}). The decrease in the number of outlier observations in FB002 also points out an improvement in the regions in which the innovations are larger, as can be deduced from Fig. 9.

On the last day of experiments (Fig. 9), the salinity innovations are better almost everywhere in FB002 compared to FB001. There is a significant reduction in errors in the northern basin. Assimilation decreases the number of outlier salinity observations, especially on the route between Yenikapı and Yalova. Moreover, innovations are also improved to a lesser extent in the southern basin where fewer observations are assimilated. The number of outlier temperature observations is very small in both experiments. Overall, the assimilation of temperature and salinity observations in the selected transects notably helps to correct the water column above the pycnocline.

The improvement of the analysis is also noticed in remote areas such as the A–B transect in the central basin (see Fig. 5). Figure 10 shows the difference between the truth and prior state down to 50 m depth along the A–B transect after the last assimilation cycle. Comparison of salinity differences between FB001 and FB002 reveals the improvement in the northern section down to 15 m depth. The southern part away from the coast also becomes better. The middle of the transect still has large discrepancies in both experiments at the end of 7 days. The correction in the remote area suggests a mechanism related to the outflow of the Bosphorus and the surface circulation of the Sea of Marmara. The water masses that are corrected by assimilation in the eastern basin are pushed towards the west and reduce the error.

Figure 11 depicts the RMS of the difference between NR and prior ensemble mean salinity at the first 10 m depth. It clearly supports the mechanism suggested above. The distribution of RMS of differences in the nonassimilation case shows that the Bosphorus outflow also has some capability to reduce the difference since the Black Sea water masses govern the upper layer of the Sea of Marmara (Fig. 11a and c). These two snapshots from the fifth and the last day of FB001 show the error reduction in some regions due to the dynamics. Therefore, the conclusion that the improvement is due to the assimilation is not straightforward. However, comparison of the FB001 and FB002 reveals the role of the assimilation

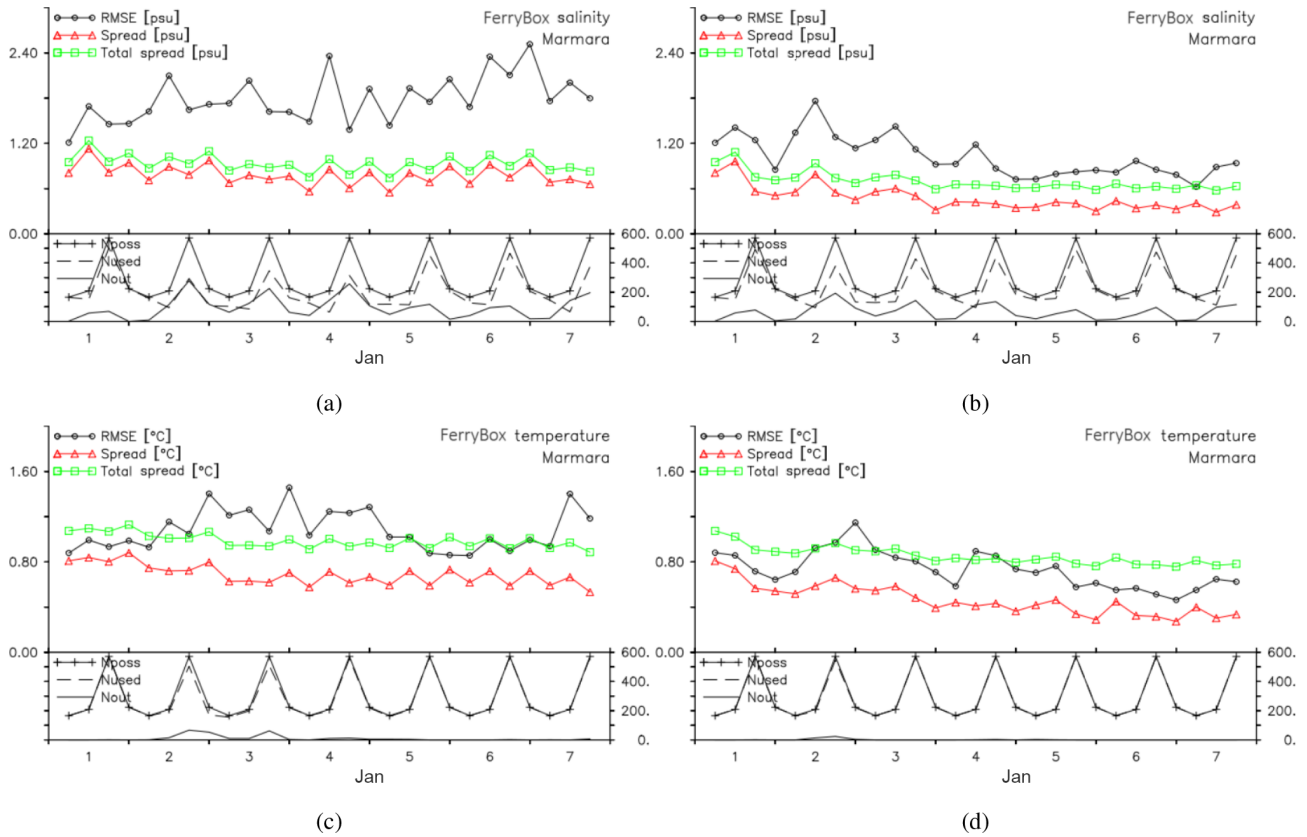


Figure 8. Time series of prior RMS of innovations, spread, and total spread of salinity (a, b) and temperature (c, d) for FB001 (a, c) and FB002 (b, d). The statistics are computed in the location of the observations used in the corresponding assimilation cycle. The spread is the square root of the variance. Total spread is the square root of the observational error added to the variance. Vertical axis shows the range of each statistics indicated in the legend. Bottom panel of each figure shows the number of available observations (N_{pos}) in each assimilation cycle. For the assimilation experiment, FB002, N_{used} and N_{out} show the number of assimilated observations and outliers, respectively. For the experiment without assimilation, FB001, they are the number of observations that would be assimilated or rejected, respectively, in that specific assimilation cycle if assimilation was performed.

of ferry tracks on the error reduction, clearly. On the fifth day, lower RMS of differences in FB002 (Fig. 11b) extends towards the easternmost part of the basin, which is absent in FB001 (Fig. 11a). The westwards propagation is more pronounced on the last day in FB002 (Fig. 11d) compared to FB001 (Fig. 11c). The central basin has lower errors almost everywhere in the north–south orientation, including the A–B transect shown before.

Temperature fields are already closer to the NR on the fifth day even in the western basin (Fig. 12). After 7 days of assimilation, the temperature error in the Bosphorus plume is significantly reduced. The southern and central basin has improvements as much as 0.5 °C locally.

Finally, Fig. 13 compares FB001 and FB002 in terms of salinity fields overlaid with corresponding circulation at 5 m depth on 7 January 2009 at 00:00 UTC. The salinity differs significantly between the two experiments, especially along the southeastern coast, while there is very little change in both qualitative and quantitative terms in the horizontal cir-

culaton, namely the current speed and direction, in the affected region that can be attributed to assimilation. The effect of assimilation is more pronounced in terms of the property fields, which alternatively indicates changes in stratification and vertical mixing along the southern coast. This can also be seen in the comparison of the experiments (Fig. 13) with the nature run (Fig. A1b), which shows that salinity in the FB002 is closer to the nature run than FB001 where the synthetic observations are assimilated. However, circulation is always more intense in the nature run compared to both experiments but both have a similar circulation pattern.

6 Summary and discussion

We have described data assimilation experiments performed in the Sea of Marmara. The main characteristics of the TSS have been summarized. For the study, a general ocean circulation model, FESOM, and an ensemble data assimilation

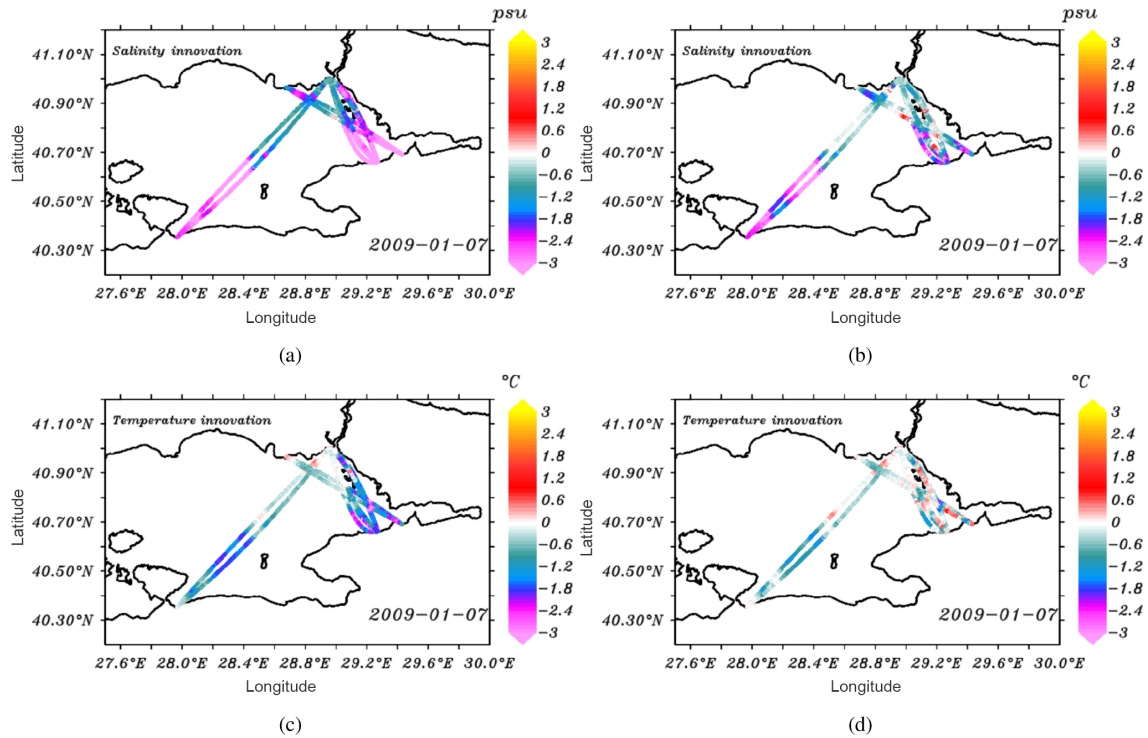


Figure 9. Horizontal distribution of salinity (a, b) and temperature (c, d) innovations along the ferry tracks on 7 January 2009 for FB001 (a, c) and FB002 (b, d). Observations with an innovation out of the range ± 3 are considered as outliers.

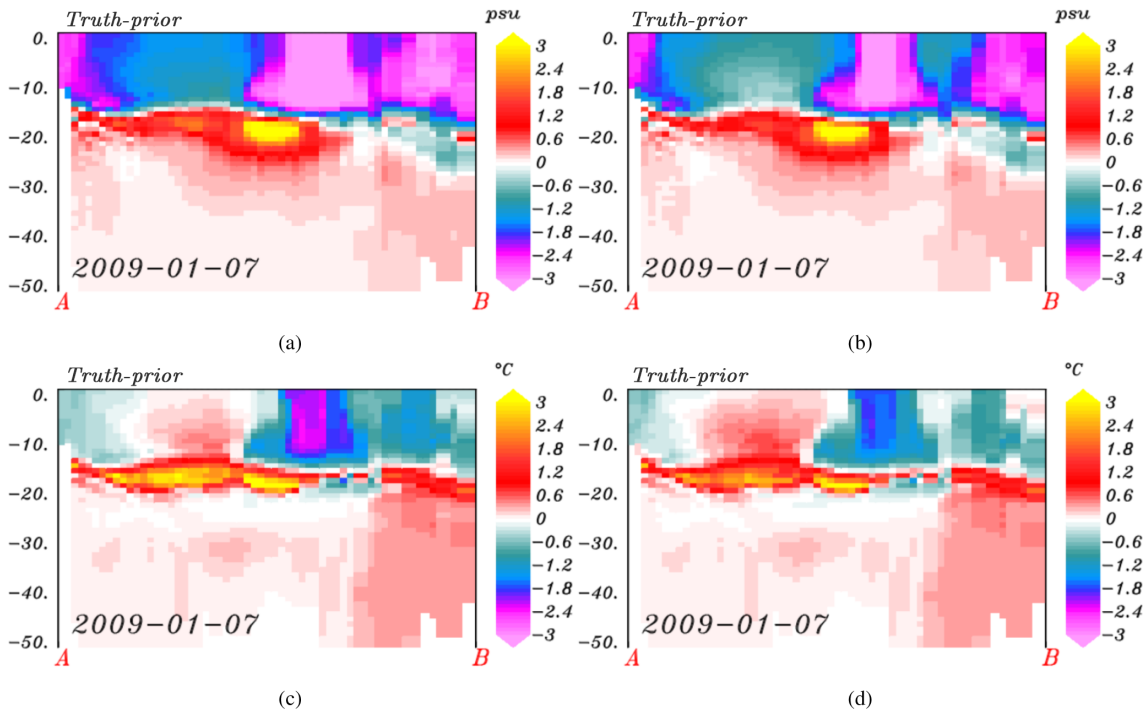


Figure 10. Vertical distribution of salinity (a, b) and temperature (c, d) difference between the NR and the prior ensemble mean along the cross section A–B (see Fig. 5) on 7 January 2009 for FB001 (a, c) and FB002 (b, d).

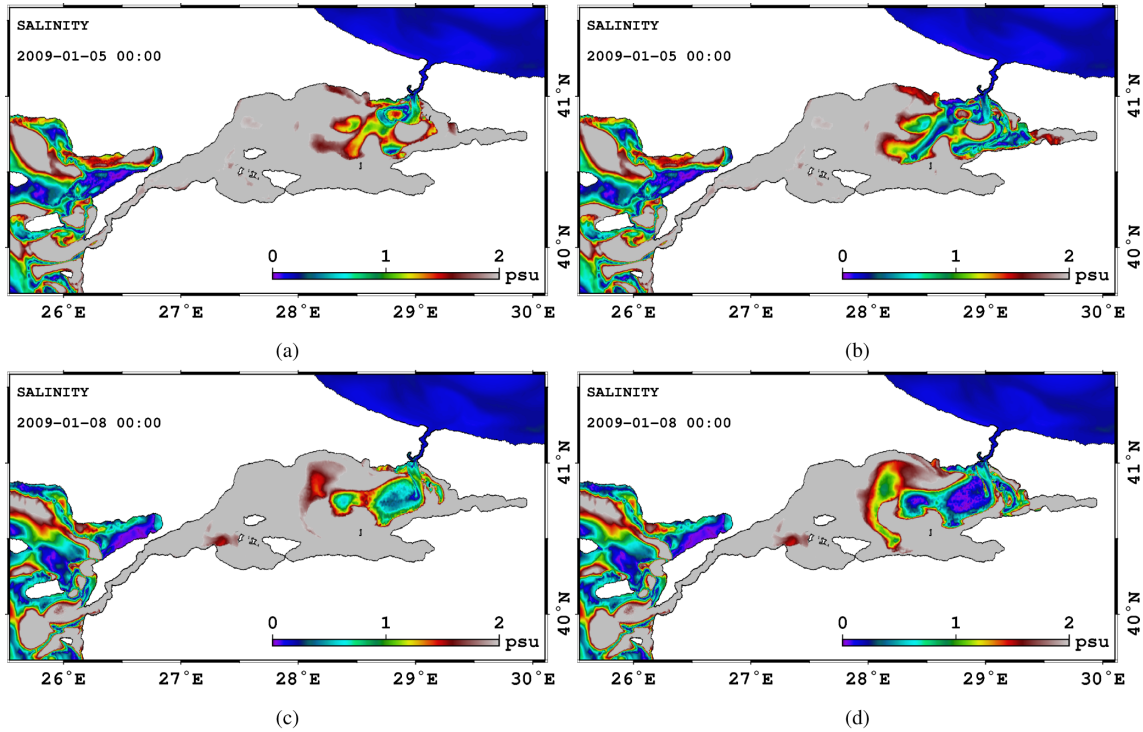


Figure 11. RMS of the difference between NR and prior ensemble mean salinity at the first 10 m. Comparison of FB001 (a, c) and FB002 (b, d) is shown for 5 January 2009 (a, b) and 8 January 2009 (c, d). RMS of difference is higher than 2 psu in the gray areas.

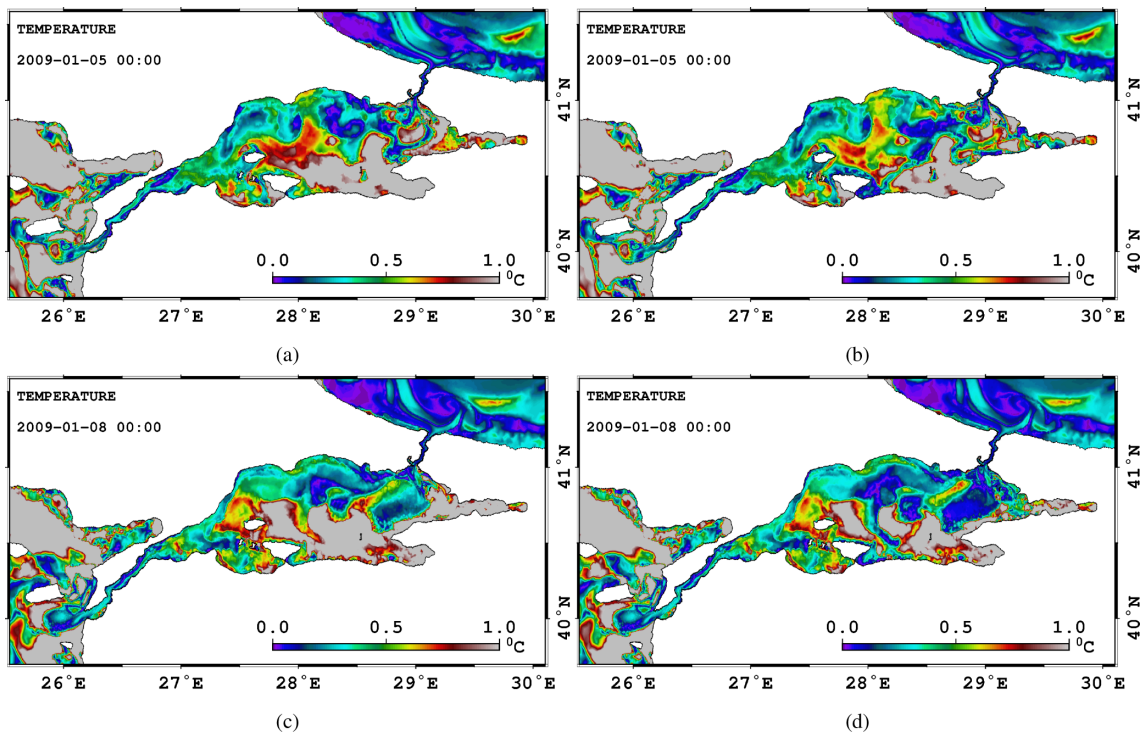


Figure 12. RMS of the difference between NR and prior temperature at the first 10 m. Comparison of FB001 (a, c) and FB002 (b, d) is shown for 5 January 2009 (a, b) and 8 January 2009 (c, d). RMS of difference is higher than 1 °C in the gray areas.

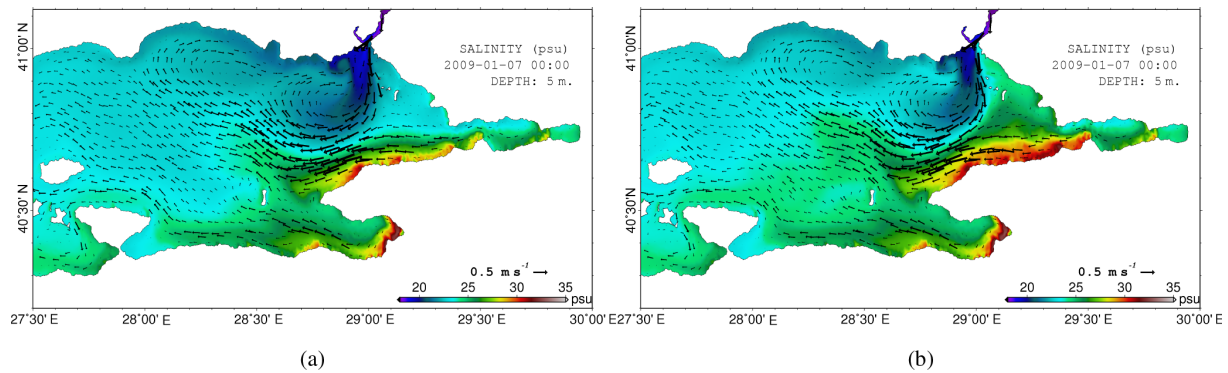


Figure 13. Salinity overlaid with current fields at 5 m depth, obtained from experiments (a) FB001 and (b) FB002 on 7 January 2009 at 00:00 UTC.

framework, DART, have been coupled. The implementation of the data assimilation scheme has been reported.

The TSS is an important water passage for the oceanography of the neighboring Black and Aegean seas. It also has important impacts on their ecosystem by maintaining the exchange of water masses and nutrients. The high population in the cities surrounding the TSS and intense marine traffic through the passages add social and economic reasons to monitor the TSS in a sustainable way.

Real observations in the TSS have been obtained by dedicated projects for short time periods or have limited spatial coverage. Moreover, the satellite measurements still have low resolution for monitoring and assimilation purposes. In this study, we proposed a sustainable marine monitoring network using the ferry lines in the eastern Sea of Marmara. We think that equipping the ferries that operate daily everyday from Istanbul to various cities around the Sea of Marmara with temperature and salinity sensors can provide immense amounts of data in both time and space. Given this motivation, we tested a FerryBox network including some of the ferry transects in the basin.

The OSSE methodology has been used to assess the impact of FerryBox measurements. We tried to satisfy the main criteria determined by approximately 40 years of experience of the atmosphere and ocean communities. However, it was still not possible to perform an observing system experiment using real observations to compare with OSSE due to the lack of data during the experiment period.

The results of the two experiments presented here are promising. We showed that the assimilation of the salinity and temperature observations significantly improve the analysis in the Sea of Marmara. The Bosphorus jet has an important role in the propagation of the error reduction towards the western basin where no data are assimilated. Moreover, the Sea of Marmara circulation helps to improve the southern basin, even for short timescales. The lower layer does not show any response to assimilation since a vertical localization around the observations around 5 m is applied to keep the impact in the upper layer as much as possible. Moreover, the stratification between the upper and lower layers is too strong, so that it prevents the interaction between the two layers. Assimilation of temperature and salinity observations does not alter the circulation in the Sea of Marmara significantly within the experiment period.

In conclusion, the results encourage further data assimilation studies in the Sea of Marmara. The investigations can be extended to different observing systems, different areas of the sea or different dynamical focuses. Moreover, we believe the unique dynamics of the system demonstrated its ability to be a good natural laboratory for future data assimilation studies.

Data availability. The link for the data will be published in the assets tab of this paper when they are made publicly available.

Appendix A

The OSSE is performed in a fraternal twin setup as discussed in Sect. 4.1. The nature run (NR) and forward model (FM) are integrated using similar model configurations, but different surface salinity boundary conditions. The NR and FM use the boundary condition (A1a) and (A1b), respectively.

$$K_v \partial_z S \Big|_{z=\eta} = \gamma (S^* - S_0) - S_{\text{corr}} \tag{A1a}$$

$$K_v \partial_z S \Big|_{z=\eta} = S_0 (E - P - R) + \gamma (S^* - S_0) - S_{\text{corr}}^* \tag{A1b}$$

In the boundary conditions (A1a) and (A1b), S_0 and S^* are the surface salinity and the reference salinity, respectively, and γ is the relaxation coefficient. S_{corr} and S_{corr}^* are correction terms applied to the salinity corresponding to boundary conditions (A1a) and (A1b), respectively. The correction term is required for mass conservation in a closed lateral boundary model and discussed extensively in Aydođdu (2017).

In Fig. A1a, the daily time series of the temperature and salinity are presented. The surface mean temperature and salinity show slight variability between 1 and 7 January 2009. The salinity field overlaid with circulation at 5 m depth on 7 January 2009 at 00:00 UTC is shown in Fig. A1b. Low-salinity water coming from the Black Sea occupies the area close to the Bosphorus Strait. High salinity near the southern and eastern coasts implies an upwelling of the Mediterranean origin water in the lower layer. The circulation in NR actually favors upwelling and is dominated mainly by westward currents with two anticyclones, one in the northern basin and the other generated by the Bosphorus jet. The NR is more saline compared to the experiments FB001 and FB002 (see Fig. 13), which are performed using the FM. This is because of the water flux term in the surface salinity boundary condition used in FM. However, both model configurations are realistic, as discussed in Aydođdu (2017).

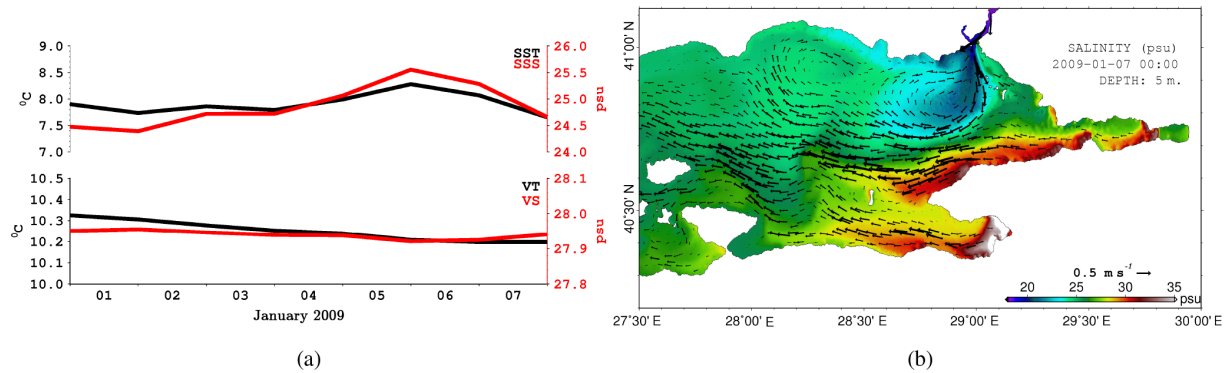


Figure A1. (a) Daily mean time series of sea surface temperature (SST), sea surface salinity (SSS), volume temperature (VT) and volume salinity (VS) in the Sea of Marmara, obtained from the nature run throughout the experiment period between 1 and 7 January 2009. (b) Salinity overlaid with current fields at 5 m depth, obtained from nature run on 7 January 2009 at 00:00 UTC.

Competing interests. The authors declare that they have no conflict of interest.

Special issue statement. This article is part of the special issue “Numerical modeling, predictability and data assimilation in weather, ocean and climate: A special issue honoring the legacy of Anna Trevisan (1946–2016)”. It is not associated with a conference.

Acknowledgements. This study is a part of the PhD thesis of Ali Aydoğdu. He is funded by Ca’ Foscari University of Venice and CMCC for his PhD and REDDA project of the Norwegian Research Council for his postdoctoral research period. The National Center for Atmospheric Research (NCAR) is a federally funded research and development center, sponsored by NSF. We are very grateful to the editor and two anonymous referees for helping us to improve the paper substantially.

Edited by: Olivier Talagrand

Reviewed by: two anonymous referees

References

- Altuok, H., Sur, H. İ., and Yüce, H.: Variation of the cold intermediate water in the Black Sea exit of the Strait of Istanbul (Bosphorus) and its transfer through the strait, *Oceanologia*, 54, 233–254, 2012.
- Anderson, J., Hoar, T., Raeder, K., Liu, H., Collins, N., Torn, R., and Avellano, A.: The data assimilation research testbed: A community facility, *B. Am. Meteorol. Soc.*, 90, 1283–1296, 2009.
- Anderson, J. L.: An ensemble adjustment Kalman filter for data assimilation, *Mon. Weather Rev.*, 129, 2884–2903, 2001.
- Anderson, J. L. and Anderson, S. L.: A Monte Carlo implementation of the nonlinear filtering problem to produce ensemble assimilations and forecasts, *Mon. Weather Rev.*, 127, 2741–2758, 1999.
- Arnold Jr., C. P. and Dey, C. H.: Observing-systems simulation experiments: Past, present, and future, *B. Am. Meteorol. Soc.*, 67, 687–695, 1986.
- Atlas, R.: Atmospheric observation and experiments to assess their usefulness in data assimilation, *J. Meteor. Soc. Jpn*, 75, 111–130, 1997.
- Aydoğdu, A.: Advanced modeling and data assimilation methods for the design of sustained marine monitoring networks, Ph.D. thesis, Università Ca’Foscari Venezia, 2017.
- Aydoğdu, A., Pinaridi, N., Pistoia, J., Martinelli, M., Belardinelli, A., and Sparnocchia, S.: Assimilation experiments for the Fishery Observing System in the Adriatic Sea, *J. Mar. Syst.*, 162, 126–136, <https://doi.org/10.1016/j.jmarsys.2016.03.002>, 2016.
- Beşiktepe, Ş. T., Sur, H. İ., Özsoy, E., Latif, M. A., Oğuz, T., and Ünlüata, Ü.: The circulation and hydrography of the Marmara Sea, *Prog. Oceanogr.*, 34, 285–334, 1994.
- Book, J. W., Jarosz, E., Chiggiato, J., and Beşiktepe, Ş.: The oceanic response of the Turkish Straits System to an extreme drop in atmospheric pressure, *J. Geophys. Res.-Oceans*, 119, 3629–3644, <https://doi.org/10.1002/2013JC009480>, 2014.
- Chiggiato, J., Jarosz, E., Book, J. W., Dykes, J., Torrisi, L., Poulain, P. M., Gerin, R., Horstmann, J., and Beşiktepe, Ş.: Dynamics of the circulation in the Sea of Marmara: Numerical modeling experiments and observations from the Turkish straits system experiment, *Ocean Dynam.*, 62, 139–159, <https://doi.org/10.1007/s10236-011-0485-5>, 2012.
- Danilov, S., Kivman, G., and Schröter, J.: A finite-element ocean model: principles and evaluation, *Ocean Modell.*, 6, 125–150, 2004.
- Gaspari, G. and Cohn, S. E.: Construction of correlation functions in two and three dimensions, *Q. J. Roy. Meteorol. Soc.*, 125, 723–757, 1999.
- Grayek, S., Staneva, J., Schulz-Stellenfleth, J., Petersen, W., and Stanev, E. V.: Use of FerryBox surface temperature and salinity measurements to improve model based state estimates for the German Bight, *J. Mar. Syst.*, 88, 45–59, <https://doi.org/10.1016/j.jmarsys.2011.02.020>, 2011.
- Gürses, Ö., Aydoğdu, A., Pinaridi, N., and Özsoy, E.: A finite element modeling study of the Turkish Straits System, in: *The Sea of Marmara – Marine Biodiversity, Fisheries, Conservations and Governance*, edited by: Öztürk, B., Çağatay, M. N., Balkis, N., Balkis, N., and Öztürk, B., 169–184, TUDAV Publication, 2016.
- Halliwel Jr., G., Srinivasan, A., Kourafalou, V., Yang, H., Willey, D., Le Hénaff, M., and Atlas, R.: Rigorous evaluation of a fraternal twin ocean OSSE system for the Open Gulf of Mexico, *J. Atmos. Ocean. Tech.*, 31, 105–130, 2014.
- Halliwel Jr., G., Kourafalou, V., Le Hénaff, M., Shay, L., and Atlas, R.: OSSE impact analysis of airborne ocean surveys for improving upper-ocean dynamical and thermodynamical forecasts in the Gulf of Mexico, *Prog. Oceanogr.*, 130, 32–46, <https://doi.org/10.1016/j.pocean.2014.09.004>, 2015.
- Hoteit, I., Hoar, T., Gopalakrishnan, G., Collins, N., Anderson, J., Cornuelle, B., Köhl, A., and Heimbach, P.: A MITgcm/DART ensemble analysis and prediction system with application to the Gulf of Mexico, *Dynam. Atmos. Ocean.*, 63, 1–23, 2013.
- Houtekamer, P. L. and Mitchell, H. L.: Data assimilation using an ensemble Kalman filter technique, *Mon. Weather Rev.*, 126, 796–811, 1998.
- Huang, R. X.: Real Freshwater Flux as a Natural Boundary Condition for the Salinity Balance and Thermohaline Circulation Forced by Evaporation and Precipitation, *J. Phys. Oceanogr.*, 23, 2428–2446, [https://doi.org/10.1175/1520-0485\(1993\)023<2428:RFFAAN>2.0.CO;2](https://doi.org/10.1175/1520-0485(1993)023<2428:RFFAAN>2.0.CO;2), 1993.
- Hüsrevoğlu, S.: Modeling Of The Dardanelles Strait Lower-layer Flow Into The Marmara Sea, Master’s thesis, Institute of Marine Sciences, METU, 1998.
- Jarosz, E., Teague, W. J., Book, J. W., and Beşiktepe, Ş.: On flow variability in the Bosphorus Strait, *J. Geophys. Res.-Oceans* (1978–2012), 116, C08038, <https://doi.org/10.1029/2010JC006861>, 2011.
- Jarosz, E., Teague, W. J., Book, J. W., and Beşiktepe, Ş.: Observations on the characteristics of the exchange flow in the Dardanelles Strait, *J. Geophys. Res.-Oceans*, 117, c11012, <https://doi.org/10.1029/2012JC008348>, 2012.
- Karspeck, A. R., Yeager, S., Danabasoglu, G., Hoar, T., Collins, N., Raeder, K., Anderson, J., and Tribbia, J.: An Ensemble Adjustment Kalman Filter for the CCSM4 Ocean Component, *J. Climate*, 26, 7392–7413, <https://doi.org/10.1175/JCLI-D-12-00402.1>, 2013.

- Korres, G., Ntoumas, M., Potiris, M., and Petihakis, G.: Assimilating Ferry Box data into the Aegean Sea model, *J. Mar. Syst.*, 140, 59–72, <https://doi.org/10.1016/j.jmarsys.2014.03.013>, 2014.
- Masutani, M., Schlatter, T. W., Errico, R. M., Stoffelen, A., Andersson, E., Lahoz, W., Woollen, J. S., Emmitt, G. D., Riishøjgaard, L.-P., and Lord, S. J.: Observing system simulation experiments, in: *Data Assimilation*, 647–679, Springer, 2010.
- Özsoy, E., Di Iorio, D., Gregg, M. C., and Backhaus, J. O.: Mixing in the Bosphorus Strait and the Black Sea continental shelf: observations and a model of the dense water outflow, *J. Mar. Syst.*, 31, 99–135, 2001.
- Petersen, W.: FerryBox systems: State-of-the-art in Europe and future development, *J. Mar. Syst.*, 140, Part A, 4–12, <https://doi.org/10.1016/j.jmarsys.2014.07.003>, 2014.
- Raeder, K., Anderson, J. L., Collins, N., Hoar, T. J., Kay, J. E., Lauritzen, P. H., and Pincus, R.: DART/CAM: An Ensemble Data Assimilation System for CESM Atmospheric Models, *J. Climate*, 25, 6304–6317, <https://doi.org/10.1175/JCLI-D-11-00395.1>, 2012.
- Sannino, G., Sözer, A., and Özsoy, E.: A high-resolution modelling study of the Turkish Straits System, *Ocean Dynam.*, 67, 397–432, <https://doi.org/10.1007/s10236-017-1039-2>, 2017.
- Schwartz, C. S., Romine, G. S., Sobash, R. A., Fossell, K. R., and Weisman, M. L.: NCAR's Experimental Real-Time Convection-Allowing Ensemble Prediction System, *Weather Forecast.*, 30, 1645–1654, <https://doi.org/10.1175/WAF-D-15-0103.1>, 2015.
- Seppälä, J., Ylöstalo, P., Kaitala, S., Hällfors, S., Raateoja, M., and Maunula, P.: Ship-of-opportunity based phycocyanin fluorescence monitoring of the filamentous cyanobacteria bloom dynamics in the Baltic Sea, *Estuarine, Coast. Shelf Sci.*, 73, 489–500, <https://doi.org/10.1016/j.ecss.2007.02.015>, 2007.
- Sørensen, K., Grung, M., and Röttgers, R.: An intercomparison of in vitro chlorophyll a determinations for MERIS level 2 data validation, *Int. J. Remote Sens.*, 28, 537–554, <https://doi.org/10.1080/01431160600815533>, 2007.
- Sözer, A. and Özsoy, E.: Modeling of the Bosphorus exchange flow dynamics, *Ocean Dynam.*, 1–23, <https://doi.org/10.1007/s10236-016-1026-z>, 2017.
- Stanev, E. V., Grashorn, S., and Zhang, Y. J.: Cascading ocean basins: numerical simulations of the circulation and interbasin exchange in the Azov-Black-Marmara-Mediterranean Seas system, *Ocean Dynam.*, 1–23, 2017.
- Tuğrul, S., Beşiktepe, T., and Salihođlu, I.: Nutrient exchange fluxes between the Aegean and Black Seas through the Marmara Sea, *Mediterranean Marine Science*, 3, 33–42, 2002.
- Ünlüata, Ü., Ođuz, T., Latif, M., and Özsoy, E.: On the physical oceanography of the Turkish Straits, in: *The physical oceanography of sea straits*, 25–60, Springer, 1990.
- Wang, Q., Danilov, S., and Schröter, J.: Finite element ocean circulation model based on triangular prismatic elements, with application in studying the effect of topography representation, *J. Geophys. Res.-Oceans* (1978–2012), 113, C05015, <https://doi.org/10.1029/2007JC004482>, 2008.